SCIENCE CHINA
Information Sciences

• RESEARCH PAPER •

October 2021, Vol. 64 202202:1–202202:12
https://doi.org/10.1007/s11432-020-3145-0

Adaptive control with saturation-constrainted observations for drag-free satellites — a set-valued identification approach

Shuping TAN[1], Jin GUO[2], Yanlong ZHAO[3] & Jifeng ZHANG[3*]

[1]*Science and Technology on Space Intelligent Control Laboratory, Beijing Institute of Control Engineering, Beijing* 100190*, China;*
[2]*School of Automation and Electrical Engineering, University of Science and Technology Beijing, Beijing* 100083*, China;*
[3]*Key Laboratory of Systems and Control, Academy of Mathematics and Systems Science, Chinese Academy of Sciences, Beijing* 100190*, China*

Received 9 July 2020/Revised 6 October 2020/Accepted 27 November 2020/Published online 15 September 2021

Abstract The high-accuracy drag-free control is one of the key technologies for gravity gradient satellites. Since the range of the gravity gradiometer is limited, the measurement is subject to the saturation constraint. This paper introduces a design method of the adaptive drag-free control law by employing the set-valued identification approach. By inserting several thresholds in the constrained interval, the output observation is transformed into the set-valued information under different thresholds, based on which and the weighted optimization technique the identification algorithm for the unknown parameter is constructed. The adaptive drag-free control law is designed via the certainty equivalence principle. It is shown that the identification algorithm is strongly convergent and the convergence rate of the estimation error is obtained. The performance of the closed-loop system is analyzed, and the asymptotic optimality of the adaptive controller is proved. The numerical simulation is included to verify the effectiveness of the main results.

Keywords drag-free satellite, saturation constraint, adaptive control, set-valued identification

Citation Tan S P, Guo J, Zhao Y L, et al. Adaptive control with saturation-constrainted observations for drag-free satellites — a set-valued identification approach. Sci China Inf Sci, 2021, 64(10): 202202, https://doi.org/10.1007/s11432-020-3145-0

1 Introduction

The gravity field and its changes reflect the spatial distribution and the movement of the earth's surface and interior material, and determine the fluctuation of the geoid. Therefore, finding the fine structure of the earth's gravity field is not only the needs of geodesy, oceanography, seismology, space science, astronomy, planetary science, deep space exploration, and national defense construction, but also provides important information for us to seek resources and protect the environment and predict disasters [1, 2].

The use of satellite technology to detect the earth's gravity field is not affected by the terrain and other natural conditions, which opens a new and effective way to solve the problem of global gravity measurement with high coverage rate, high precision, high spatial resolution and high time repetition rate. The drag-free control is one of the key technologies for gravity gradient satellites. Its main aim is to provide a flight environment for gravity gradiometer under the pure gravity and meet the technical requirements of payload normal operation for the platform, by controlling propellers to generate appropriate thrust to offset the non-conservative forces such as atmospheric resistance or solar pressure. Owing to the significance of both theory and practice, the research on the drag-free control has attracted wide attention and many important achievements have been made [3–10].

Lange systematically studied drag-free satellites, and proposed the comprehensive application of the drag-free satellite and its different forms. In his doctoral dissertation [3] in 1964, the motion equation of

* Corresponding author (email: jif@iss.ac.cn)

© Science China Press and Springer-Verlag GmbH Germany, part of Springer Nature 2021

a 9-degree-of-freedom (9-DOF) drag-free satellite was derived, and its dynamics and control technology were investigated. Ref. [4] decoupled the multi-input and multi-output system of a drag-free satellite, then used the traditional proportion-integration-differentiation (PID) controller to control each single-input and single-output system, and the genetic algorithm was used to optimize the gain of the controller. Ref. [5] considered the periodic change of driving ability caused by the change of magnetic field along the orbit direction and designed a new linear quadratic regulator controller with robustness. Ref. [6] applied the embedded model control to the design of drag-free and attitude control for a gravity-field and ocean-circulation-explorer (GOCE) satellite. Ref. [7] designed an H_∞ controller by using linear matrix inequality multi-objective optimization method. Many constraints were taken into account to ensure the realization of the drag-free control task of the GOCE satellite and to make the controller robust. Using the quantitative feedback theory, Ref. [8] designed and tuned the drag-free and attitude controllers used on board in the Laser Interferometer Space Antenna (LISA) pathfinder science mission. Ref. [9] employed the model predictive technology to deal with the constraints of drag-free satellite control. Considering the actual capacity of the actuator, the quadratic programming method was used to calculate the predictive control quantity. Ref. [10] introduced an active disturbance rejection control strategy to design the controller for drag-free satellites.

The gravity gradiometer has high observation accuracy, but its range is relatively small. The acceleration caused by non-conservative forces can exceed the observation range. Consequently, the observation information is subject to saturation constraints, which restricts the design of the drag-free control law to a large extent. The observation under saturation constraints is made up of two types of information. One type is the accurate information (with some additive measurement noise) in the constrained interval, and the other is the set-valued information outside the constrained interval. This is essentially different from the one considered by the conventional control theory [11–13]. The information provided by the observation under saturation constraints is relatively limited, and is substantially non-linear with respect to the actual system input, state, and controlled output. The conventional methods developed for linear and non-linear systems cannot be used directly. This makes us have to develop new system identification and controller design methods according to the characteristics of saturation-constrainted data.

In recent years, the identification theory with set-valued observations has been greatly developed [14–20], which offers a possible way to deal with the identification problem under saturation constraints. Many important results have been obtained and some effective techniques have been proposed [21–28]. Under the full-rank periodic input, Ref. [21] studied a series of problems such as the optimal identification error and the time and space complexity of set-valued output systems by using an empirical measure method, and discussed the influence of disturbance and unmodeled dynamics on identification precision. Ref. [22] studied a parameter estimation problem of networked linear systems with fixed-rate quantization under the minimum mean square error criterion. Ref. [23] considered parameter estimation with only binary measurements of the input and output signals available, and several estimation schemes based on empirical measures and stochastic approximation algorithms were proposed and analysed. Based on the stationary ergodic normal input, Ref. [24] proposed a weighted least squares algorithm to estimate the unknown parameters of FIR systems with binary-valued observations. Ref. [25] studied the iterative estimation problem of systems with binary-valued observations via the expectation maximization method, and the convergence rate of the algorithm was also given. Along with the gradual development and improvement of identification methods the adaptive control for systems with set-valued observations has also been addressed accordingly. Under binary-valued observations, Refs. [26, 27] handled the adaptive tracking control of a class of first-order systems with fixed and variable thresholds respectively. The design method of the adaptive control law was given, and the performance of the closed-loop system was analyzed. For FIR systems with set-valued observations and periodic target signals, Ref. [28] designed a two-scale adaptive tracking controller based on the empirical measure method and certainty equivalence principle. Its asymptotic optimality was proved, and the convergence, the convergence rate, and the asymptotic efficiency of parameter estimation were obtained.

This paper proposes a set-valued identification-based adaptive controller design method for drag-free control under saturation-constrainted observations. By setting several thresholds in the constrained interval, the observation is transformed into set-valued information under different thresholds. According to the set-valued information provided by every thresholds, innovation sequences are constructed and a set of stochastic approximation identification algorithms are derived. They are weighted and generate a recursive projection identification algorithm to estimate the unknown parameter. Via the certainty equivalence principle, the adaptive drag-free control law is designed. The strong convergence of the

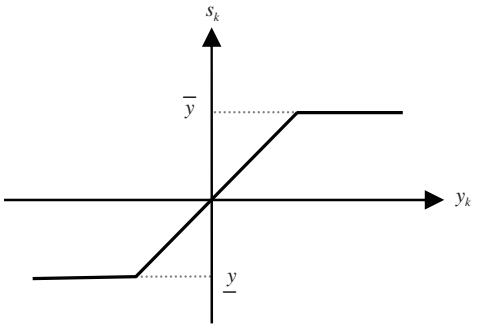

Figure 1 Saturation-constrainted observations.

identification algorithm is proved. Using the estimation method of the sum of weighted martingale difference sequence (MDS), the convergence rate of estimation error is given. The performance of the closed-loop system is analyzed, and the asymptotic optimality of the adaptive controller is shown by the law of large numbers for the MDS.

The rest of the paper is organized as follows. Section 2 describes the drag-free control problem with saturation constraints. Section 3 gives the identification algorithm and the adaptive control law. Section 4 discusses the performance of the identification algorithm and the closed-loop system, including the convergence, the convergence rate, and the asymptotic optimality of the adaptive controller. Section 5 is a numerical simulation that shows the effectiveness of the main results. Section 6 summarizes the finding of the paper and looks forward to future research work.

2 Problem formulation

Consider the motion of a drag-free satellite along the tangent direction of its orbit:

$$P - R = Ma, \quad R = \frac{1}{2}C\rho S v^2, \tag{1}$$

where $P \in [P_{\min}, P_{\max}]$ is the thrust and depends on the performance of the actuator, $P_{\min}$ means the minimum thrust and $P_{\max}$ is the maximum one that can be achieved; R is the atmospheric drag; a is the residual acceleration; M is the quality of the satellite; v is the speed of the satellite along the tangent direction and can be obtained; C is the atmospheric drag coefficient, ρ is atmospheric density, S is the windward area. All of these are unknown parameters. Letting $y = a$, according to (1), we can get

$$y = \frac{P}{M} - \frac{v^2}{2M}C\rho S. \tag{2}$$

Let $u = \frac{P}{M}$, $\alpha = -\frac{v^2}{2M}$, $\theta = C\rho S$, and use k to indicate the sampling time. Then it is known that

$$y_k = \begin{pmatrix} u_k & \alpha_k \end{pmatrix} \begin{pmatrix} 1 \\ \theta \end{pmatrix} + d_k. \tag{3}$$

Consequently, u_k is the control input that can be designed, α_k is a measurable variable, θ is the unknown parameter to be identified, and d_k is the system noise.

Owing to the range limitation of the gravity gradiometer, the observation of y_k is limited by the saturation constraint. That is, there is a saturation constraint interval $[\underline{y}, \overline{y}]$ such that the value of y_k can be observed only when y_k is in the interval. Thus, the available information is represented by the following saturation function (as shown in Figure 1):

$$s_k = \mathcal{S}(y_k) = \begin{cases} \underline{y}, & y_k < \underline{y}, \\ y_k, & y_k \in [\underline{y}, \overline{y}], \\ \overline{y}, & y_k > \overline{y}. \end{cases} \tag{4}$$

The aim of this paper is to design u_k based on s_k to ensure that y_k is in the middle of $[\underline{y}, \overline{y}]$, i.e., $y^* = \frac{1}{2}(\underline{y} + \overline{y})$, and minimize the following index:

$$J_k = \frac{1}{k}\sum_{j=1}^{k}(y_j - y^*)^2. \tag{5}$$

To do this, we first need to construct an identification algorithm to estimate θ, then design an adaptive control law based on the certainty equivalence principle, and finally complete the performance analysis of the closed-loop system.

Assumption 1. The system noise $\{d_k\}$ is an independent and identically distributed (i.i.d.) Gaussian random variable sequence, where the mean is 0 and the variance is σ^2, i.e., $d_k \sim \mathcal{N}(0, \sigma^2)$. Let $F(\cdot)$ denote its distribution function and $f(\cdot)$ denote the density function.

Assumption 2. There exist two constants $\overline{\theta}$ and $\underline{\theta}$ such that $\overline{\theta} > \underline{\theta} > 0$ and $\theta \in [\underline{\theta},\ \overline{\theta}] := \Theta$.

Remark 1. In view of (4), one can see that s_k is made up of two types of information. One type is the accurate information in $[\underline{y}, \overline{y}]$, and the other is the set-valued information outside $[\underline{y}, \overline{y}]$. How to deal with such information is the main difference from the traditional methods.

3 The identification algorithm and adaptive control law

For a given positive integer $m \geqslant 2$, we take $m-2$ real numbers between $\underline{y}$ and $\overline{y}$, denoted by $T_2, \ldots, T_{m-1}$ from small to large, that is,

$$\underline{y} = T_1 < T_2 < \cdots < T_{m-1} < T_m = \overline{y},$$

where $T_1 = \underline{y}$ and $T_m = \overline{y}$. Then, m sequences $\{s_k^{\{i\}}\}$ can be constructed by use of the observation sequence $\{s_k\}$, which leads to

$$\begin{aligned} &s_k^{\{i\}} = I_{\{s_k \leqslant T_i\}}, \quad i = 1, \ldots, m-1, \\ &s_k^{\{m\}} = 1 - I_{\{s_k = \overline{y}\}}, \end{aligned} \tag{6}$$

where $I_{\{z \in A\}}$ represents the indicator function of the set A, i.e., $I_{\{z \in A\}} = 1$ if $z \in A$; otherwise, $I_{\{z \in A\}} = 0$.

We introduce the following algorithm to estimate θ, in which $\{s_k^{\{i\}}\}$ is used to get $\widehat{\theta}_k^{\{i\}}$, $i = 1, \ldots, m$, and then they are weighted to get the estimate $\widehat{\theta}_k$ of θ at time k,

$$\widehat{\theta}_k = \sum_{i=1}^{m} \nu_i \widehat{\theta}_k^{\{i\}}, \tag{7}$$

$$\widehat{\theta}_k^{\{i\}} = \Pi_\Theta\left\{\widehat{\theta}_{k-1}^{\{i\}} + \beta_i \frac{\alpha_k}{k}\widetilde{s}_k^{\{i\}}\right\}, \tag{8}$$

$$\widetilde{s}_k^{\{i\}} = F\left(T_i - u_k - \alpha_k \widehat{\theta}_{k-1}^{\{i\}}\right) - s_k^{\{i\}}, \tag{9}$$

where $\nu_1, \ldots, \nu_m$ are weighting coefficients that satisfy $\sum_{i=1}^{m} \nu_i = 1$; $\beta_i > 0$ is a given constant used to adjust the convergence rate; the initial value $\widehat{\theta}_0^{\{i\}}$ can be arbitrarily selected in Θ; $\Pi_\Theta(\cdot)$ is the projection operator, i.e., $\Pi_\Theta(z) = \operatorname{argmin}_{\omega \in \Theta}|\omega - z|$; $F(\cdot)$ is the distribution function of the noise, given by Assumption 1.

When θ is known, the control law that minimizes the index (5) should satisfy

$$\begin{pmatrix} u_k & \alpha_k \end{pmatrix}\begin{pmatrix} 1 \\ \theta \end{pmatrix} = y^*, \tag{10}$$

$$u_k \in U = \left[\frac{P_{\min}}{M}, \frac{P_{\max}}{M}\right]. \tag{11}$$

If the equations above are compatible (i.e., the solution of (10) satisfies the constraint in (11)), then $u_k = y^* - \alpha_k\theta$. Substituting it into (3), the closed-loop equation can be obtained:

$$J_k = \frac{1}{k}\sum_{j=1}^{k}(y_j - y^*)^2 = \frac{1}{k}\sum_{j=1}^{k} d_j^2 \to \sigma^2 \quad \text{a.s.} \quad k \to \infty.$$

When θ is unknown, according to the certainty equivalence principle, θ is replaced by $\widehat{\theta}_{k-1}$ in (10). Together with (11) the adaptive control law is designed as follows:

$$u_k = \Pi_U \left\{ y^* - \alpha_k \widehat{\theta}_{k-1} \right\}. \tag{12}$$

Remark 2. In (6), the saturation-constrainted observation s_k is transformed into a set of set-valued information by inserting several thresholds in $[\underline{y}, \overline{y}]$. The advantage of this approach is that one can uniformly deal with the accurate information in $[\underline{y}, \overline{y}]$ and the set-valued information outside $[\underline{y}, \overline{y}]$, which makes it more convenient to fully utilize set-valued identification algorithms. However, it may waste the observation information since some accurate information is reduced to set-valued information. An effective way to remedy this deficiency is to design enough thresholds according to the desired control accuracy. Another way is to employ the maximum likelihood estimation method for obtaining the identification algorithm.

Remark 3. In (7)–(9), every $\widehat{\theta}_k^{\{i\}}$ is generated independently. In practical application, they can be cross-updated, that is, Eqs. (8) and (9) use $\widehat{\theta}_{k-1}$ instead of $\widehat{\theta}_{k-1}^{\{i\}}$ to generate $\widehat{\theta}_k^{\{i\}}$. This cross-updated algorithm may have a faster convergence rate, which will be shown in Section 5.

4 Performance of the identification algorithm and the closed-loop system

Lemma 1 ([26])**.** Suppose that $\{x_k, k \geqslant 1\}$ is a sequence of real numbers such that for all sufficiently large k,

$$x_k \leqslant \left(1 - \frac{\lambda}{k+a}\right) x_{k-1} + \frac{\mu}{(k-1)^{2+\delta}},$$

where $a \in \{x : x \in \mathbb{R}, x \neq -1, -2, \ldots\}$, $\lambda > 0$, $\delta \geqslant 0$. Then

$$x_k = \begin{cases} O\left(\dfrac{1}{k^{\lambda}}\right), & 0 < \lambda < 1 + \delta, \\ O\left(\dfrac{\log k}{k^{1+\delta}}\right), & \lambda = 1 + \delta, \\ O\left(\dfrac{1}{k^{1+\delta}}\right), & \lambda > 1 + \delta. \end{cases}$$

Lemma 2 (Lemma 2.2 in [29])**.** Let $\{a_k, \mathscr{F}_k\}$, $\{b_k, \mathscr{F}_k\}$ be two non-negative adaptive sequences. If $\mathrm{E}[a_k|\mathscr{F}_{k-1}] \leqslant a_{k-1} + b_{k-1}$ and $\mathrm{E}\sum_{k=1}^{\infty} b_k < \infty$, then a_k almost everywhere converges to a finite limit.

Let $\widetilde{\theta}_k^{\{i\}} = \widehat{\theta}_k^{\{i\}} - \theta$, $k = 0, 1, 2, \ldots$ denote the estimation error, and $\mathscr{F}_k$ denote the σ-algebra generated by $d_1, \ldots, d_k$.

Theorem 1. Consider system (3) under saturation-constrainted observation (4). If

(i) Assumptions 1 and 2 hold,

(ii) there exist constants $\overline{\alpha} > \underline{\alpha} > 0$ such that $\underline{\alpha} \leqslant |\alpha_k| \leqslant \overline{\alpha}$,

(iii) u_k is $\mathscr{F}_{k-1}$-measurable, and there exists a constant $\overline{u} > 0$ such that $|u_k| \leqslant \overline{u}$,

then $\widehat{\theta}_k$ given by (7) strongly converges to the true value, i.e., $\widehat{\theta}_k \to \theta$, with probability 1 (w.p.1) $k \to \infty$.

Proof. For $i = 1, \ldots, m-1$, from (4) it can be seen that $s_k \leqslant T_i$ if and only if $y_k \leqslant T_i$. According to (3), (6) and Assumption 1, we can get

$$\begin{aligned} \mathrm{E}\left[s_k^{\{i\}}|\mathscr{F}_{k-1}\right] &= \Pr(s_k \leqslant T_i|\mathscr{F}_{k-1}) \\ &= \Pr(y_k \leqslant T_i|\mathscr{F}_{k-1}) \\ &= \Pr(u_k + \alpha\theta + d_k \leqslant T_i|\mathscr{F}_{k-1}) \\ &= F(T_i - u_k - \alpha\theta) \end{aligned}$$

and

$$\mathrm{E}\left[s_k^{\{m\}}|\mathscr{F}_{k-1}\right] = \mathrm{E}\left[1 - I_{\{s_k = \overline{y}\}}|\mathscr{F}_{k-1}\right]$$

$$
\begin{aligned}
&= 1 - \Pr(s_k = \overline{y}|\mathscr{F}_{k-1}) \\
&= 1 - \Pr(y_k > \overline{y}|\mathscr{F}_{k-1}) \\
&= F(\overline{y} - u_k - \alpha\theta) \\
&= F(T_m - u_k - \alpha\theta).
\end{aligned}
$$

Therefore, it follows that

$$
\mathrm{E}\left[s_k^{\{i\}}|\mathscr{F}_{k-1}\right] = F(T_i - u_k - \alpha\theta), \quad i = 1, \ldots, m. \tag{13}
$$

By (8) and the property of the projection operator, it can be seen that

$$
\begin{aligned}
\left(\widetilde{\theta}_k^{\{i\}}\right)^2 &= \left(\widehat{\theta}_k^{\{i\}} - \theta\right)^2 \\
&= \left(\Pi_\Theta\left\{\widehat{\theta}_{k-1}^{\{i\}} + \beta_i \frac{\alpha_k}{k}\widetilde{s}_k^{\{i\}}\right\} - \Pi_\Theta\left\{\theta\right\}\right)^2 \\
&\leqslant \left(\left\{\widehat{\theta}_{k-1}^{\{i\}} + \beta_i \frac{\alpha_k}{k}\widetilde{s}_k^{\{i\}}\right\} - \theta\right)^2 \\
&= \left(\widetilde{\theta}_{k-1}^{\{i\}} + \beta_i \frac{\alpha_k}{k}\widetilde{s}_k^{\{i\}}\right)^2.
\end{aligned}
$$

Considering $|\widetilde{s}_k^{\{i\}}| \leqslant 2$ and the above, one can have

$$
\left(\widetilde{\theta}_k^{\{i\}}\right)^2 \leqslant \left(\widetilde{\theta}_{k-1}^{\{i\}}\right)^2 + 2\beta_i \frac{\alpha_k \widetilde{\theta}_{k-1}^{\{i\}}}{k}\widetilde{s}_k^{\{i\}} + \beta_i^2 \frac{4\alpha_k^2}{k^2}. \tag{14}
$$

Taking the conditional expectation with respect to $\mathscr{F}_{k-1}$ on the both sides of the above, and combining (9) and (13), we have

$$
\begin{aligned}
&\mathrm{E}\left[(\widetilde{\theta}_k^{\{i\}})^2|\mathscr{F}_{k-1}\right] \\
&\leqslant \left(\widetilde{\theta}_{k-1}^{\{i\}}\right)^2 + 2\beta_i \frac{\alpha_k \widetilde{\theta}_{k-1}^{\{i\}}}{k}\mathrm{E}\left[\widetilde{s}_k^{\{i\}}|\mathscr{F}_{k-1}\right] + \beta_i^2 \frac{4\alpha_k^2}{k^2} \\
&= \left(\widetilde{\theta}_{k-1}^{\{i\}}\right)^2 + 2\beta_i \frac{\alpha_k \widetilde{\theta}_{k-1}^{\{i\}}}{k}\left(F\left(T_i - u_k - \alpha_k \widehat{\theta}_{k-1}^{\{i\}}\right) - \mathrm{E}\left[s_k^{\{i\}}|\mathscr{F}_{k-1}\right]\right) + \beta_i^2 \frac{4\alpha_k^2}{k^2} \\
&= \left(\widetilde{\theta}_{k-1}^{\{i\}}\right)^2 + 2\beta_i \frac{\alpha_k \widetilde{\theta}_{k-1}^{\{i\}}}{k}\left(F\left(T_i - u_k - \alpha_k \widehat{\theta}_{k-1}^{\{i\}}\right) - F(T_i - u_k - \alpha_k\theta)\right) + \beta_i^2 \frac{4\alpha_k^2}{k^2}.
\end{aligned} \tag{15}
$$

By virtue of the differential mean value theorem, there exists $\xi_k^{\{i\}}$ between $T_i - u_k - \alpha_k \widehat{\theta}_{k-1}^{\{i\}}$ and $T_i - u_k - \alpha_k\theta$ such that

$$
\begin{aligned}
&F\left(T_i - u_k - \alpha_k \widehat{\theta}_{k-1}^{\{i\}}\right) - F(T_i - u_k - \alpha\theta) \\
&\quad = F'\left(\xi_k^{\{i\}}\right)\left[\left(T_i - u_k - \alpha_k \widehat{\theta}_{k-1}^{\{i\}}\right) - (T_i - u_k - \alpha\theta)\right] \\
&\quad = -f\left(\xi_k^{\{i\}}\right)\alpha_k \widetilde{\theta}_{k-1}^{\{i\}},
\end{aligned} \tag{16}
$$

and

$$
|\xi_k^{\{i\}}| \leqslant |T_i| + \overline{u} + \overline{\alpha}\overline{\theta} := \overline{\xi}^{\{i\}}. \tag{17}
$$

Since $f(\cdot)$ is an even function and monotonically decreasing on $[0, \infty)$, with (15) and $\underline{\alpha} \leqslant |\alpha_k| \leqslant \overline{\alpha}$ we have

$$
\begin{aligned}
\mathrm{E}\left[\left(\widetilde{\theta}_k^{\{i\}}\right)^2|\mathscr{F}_{k-1}\right] &\leqslant \left(\widetilde{\theta}_{k-1}^{\{i\}}\right)^2 - 2\beta_i f\left(\xi_k^{\{i\}}\right)\frac{(\alpha_k \widetilde{\theta}_{k-1}^{\{i\}})^2}{k} + \beta_i^2 \frac{4\overline{\alpha}^2}{k^2} \\
&\leqslant \left(1 - \frac{2\beta_i f(\overline{\xi}^{\{i\}})\underline{\alpha}^2}{k}\right)\left(\widetilde{\theta}_{k-1}^{\{i\}}\right)^2 + \beta_i^2 \frac{4\overline{\alpha}^2}{k^2}.
\end{aligned} \tag{18}
$$

Taking expectation on the above, it is known that

$$\mathrm{E}\left(\widetilde{\theta}_k^{\{i\}}\right)^2 = \left(1 - \frac{2\beta_i f(\overline{\xi}^{\{i\}})\underline{\alpha}^2}{k}\right)\mathrm{E}\left(\widetilde{\theta}_{k-1}^{\{i\}}\right)^2 + \beta_i^2\frac{4\overline{\alpha}^2}{k^2}.$$

Using this and Lemma 1 gives that

$$\mathrm{E}\left(\widetilde{\theta}_k^{\{i\}}\right)^2 \to 0, \quad k \to \infty. \tag{19}$$

In light of (18), it can be seen that

$$\mathrm{E}\left[\left(\widetilde{\theta}_k^{\{i\}}\right)^2 |\mathscr{F}_{k-1}\right] \leqslant \left(\widetilde{\theta}_{k-1}^{\{i\}}\right)^2 + \beta_i^2\frac{4\overline{\alpha}^2}{k^2}.$$

Note that $\sum_{k=1}^{\infty}\beta_i^2\frac{4\overline{\alpha}^2}{k^2} < \infty$. From Lemma 2, we know that $\widetilde{\theta}_k^{\{i\}}$ strongly converges to a finite limit. By (19), there is a subsequence of $\widetilde{\theta}_k^{\{i\}}$ that strongly converges to 0. Therefore, $\widetilde{\theta}_k^{\{i\}}$ strongly converges to 0, i.e., $\widehat{\theta}_k^{\{i\}} \to \theta$, w.p.1, $k \to \infty$.

Owing to $\sum_{i=1}^{m}\nu_i = 1$ and (7), it follows that $\widehat{\theta}_k \to \theta$, w.p.1 $k \to \infty$.

Lemma 3 (Theorem 1.3.10 in [30]). Consider an MDS $\{w_k, \mathscr{F}_k\}$ and an adapted process $\{h_k, \mathscr{F}_k\}$. If $\sup_k \mathrm{E}\left[|w_{k+1}|^{\alpha}|\mathscr{F}_k\right] < \infty$ a.s. $\alpha > 2$, then we have

$$\sum_{j=1}^{k} h_j w_{j+1} = O\left(H_k(\log H_k)^{\delta}\right) \quad \text{a.s.} \quad \forall\delta > \frac{1}{2}$$

with $H_k = (\sum_{j=1}^{k} h_i^2)^{1/2}$.

Theorem 2. Under the condition of Theorem 1, if

$$\beta_i > \frac{1}{2f\left(|T_i| + \overline{u} + \overline{\alpha}\overline{\theta}\right)\underline{\alpha}^2}, \quad i = 1, \ldots, m,$$

then

$$\left(\widehat{\theta}_k - \theta\right)^2 = O\left(\frac{\log k}{k}\right) \quad \text{a.s.}$$

Proof. From (9) and (14), it can be seen that

$$\begin{aligned}
&k\left(\widetilde{\theta}_k^{\{i\}}\right)^2 - (k-1)\left(\widetilde{\theta}_{k-1}^{\{i\}}\right)^2 \\
&\leqslant \left(\widetilde{\theta}_{k-1}^{\{i\}}\right)^2 + 2\beta_i\alpha_k\widetilde{\theta}_{k-1}^{\{i\}}\widetilde{s}_k^{\{i\}} + \beta_i^2\frac{4\alpha_k^2}{k} \\
&= \left(\widetilde{\theta}_{k-1}^{\{i\}}\right)^2 + 2\beta_i\alpha_k\widetilde{\theta}_{k-1}^{\{i\}}\left(F\left(T_i - u_k - \alpha_k\widehat{\theta}_{k-1}^{\{i\}}\right) - F(T_i - u_k - \alpha\theta)\right) \\
&\quad + 2\beta_i\alpha_k\widetilde{\theta}_{k-1}^{\{i\}}\left(F(T_i - u_k - \alpha_k\theta) - s_k^{\{i\}}\right) + \beta_i^2\frac{4\alpha_k^2}{k}.
\end{aligned}$$

On the basis of (16), (17) and $\underline{\alpha} \leqslant |\alpha_k| \leqslant \overline{\alpha}$, one can have

$$2\beta_i\alpha_k\widetilde{\theta}_{k-1}^{\{i\}}\left(F\left(T_i - u_k - \alpha_k\widehat{\theta}_{k-1}^{\{i\}}\right) - F(T_i - u_k - \alpha\theta)\right) \leqslant -2\beta_i f\left(\overline{\xi}^{\{i\}}\right)\underline{\alpha}^2\left(\widetilde{\theta}_{k-1}^{\{i\}}\right)^2.$$

And then

$$\begin{aligned}
&k\left(\widetilde{\theta}_k^{\{i\}}\right)^2 - (k-1)\left(\widetilde{\theta}_{k-1}^{\{i\}}\right)^2 \\
&\leqslant \left(\widetilde{\theta}_{k-1}^{\{i\}}\right)^2 - 2\beta_i f\left(\overline{\xi}^{\{i\}}\right)\underline{\alpha}^2\left(\widetilde{\theta}_{k-1}^{\{i\}}\right)^2 + 2\beta_i\alpha_k\widetilde{\theta}_{k-1}^{\{i\}}\left(F(T_i - u_k - \alpha_k\theta) - s_k^{\{i\}}\right) + \beta_i^2\frac{4\alpha_k^2}{k} \\
&= \left(1 - 2\beta_i f\left(\overline{\xi}^{\{i\}}\right)\underline{\alpha}^2\right)\left(\widetilde{\theta}_{k-1}^{\{i\}}\right)^2 + 2\beta_i\alpha_k\widetilde{\theta}_{k-1}^{\{i\}}\left(F(T_i - u_k - \alpha_k\theta) - s_k^{\{i\}}\right) + \beta_i^2\frac{4\alpha_k^2}{k},
\end{aligned}$$

which indicates that

$$k\left(\widetilde{\theta}_k^{\{i\}}\right)^2 \leqslant \left(1-2\beta_i f\left(\overline{\xi}^{\{i\}}\right)\underline{\alpha}^2\right)\sum_{j=1}^{k}\left(\widetilde{\theta}_{j-1}^{\{i\}}\right)^2 + 2\beta_i\sum_{j=1}^{k}\alpha_j\widetilde{\theta}_{j-1}^{\{i\}}\left(F(T_i-u_j-\alpha_j\theta)-s_j^{\{i\}}\right) + O(\log k). \tag{20}$$

In terms of (13), it is known that $\{F(T_i-u_k-\alpha_k\theta)-s_k^{\{i\}}, \mathscr{F}_k\}$ is an MDS. Considering $\sup_k|\alpha_k\widetilde{\theta}_{k-1}^{\{i\}}| \leqslant 2\overline{\alpha}\overline{\theta} < \infty$ and using Lemma 3, we have

$$\sum_{j=1}^{k}\alpha_j\widetilde{\theta}_{j-1}^{\{i\}}\left(F(T_i-u_j-\alpha_j\theta)-s_j^{\{i\}}\right) = O\left(\sqrt{\sum_{j=1}^{k}\left(\widetilde{\theta}_{j-1}^{\{i\}}\right)^2}\left(\log\sum_{j=1}^{k}\left(\widetilde{\theta}_{j-1}^{\{i\}}\right)^2\right)^{\delta}\right) \quad \text{a.s.} \quad \forall\delta>\frac{1}{2}.$$

Together with (20), it follows that

$$k\left(\widetilde{\theta}_k^{\{i\}}\right)^2 \leqslant \left(1-2\beta_i f\left(\overline{\xi}^{\{i\}}\right)\underline{\alpha}^2+o(1)\right)\sum_{j=1}^{k}\left(\widetilde{\theta}_{j-1}^{\{i\}}\right)^2 + O(\log k).$$

If $\beta_i > \frac{1}{2f(\overline{\xi}^{\{i\}})\underline{\alpha}^2}$, then $1-2\beta_i f(\overline{\xi}^{\{i\}})\underline{\alpha}^2 < 0$, so $k(\widetilde{\theta}_k^{\{i\}})^2 \leqslant O(\log k)$. Therefore, one can have $(\widetilde{\theta}_k^{\{i\}})^2 = O(\frac{\log k}{k})$. On account of (7), the theorem is proved.

Lemma 4 (Corollary 2 in [31]). Consider an MDS $\{w_k, \mathcal{F}_k, k \geqslant 1\}$. If $\mathrm{E}(\sum_{j=1}^{k} w_j)^2 < \infty$ and $\sum_{j=1}^{\infty}\frac{\mathrm{E}w_j^2}{j^2} < \infty$, then

$$\frac{1}{k}\sum_{j=1}^{k} w_j \to 0 \quad \text{a.s.} \quad k\to\infty.$$

Theorem 3. Consider the adaptive control law (12) and the closed-loop system (3) under saturation-constrainted observation (4). If Eq. (10) is compatible with (11), Assumptions 1 and 2 hold and there exist constants $\overline{\alpha} > \underline{\alpha} > 0$ such that $\underline{\alpha} \leqslant |\alpha_k| \leqslant \overline{\alpha}$, then the adaptive control law (12) is asymptotically optimal, i.e.,

$$J_k \to \sigma^2 \quad \text{a.s.} \quad k\to\infty.$$

Proof. Let $\Delta_j = \Pi_U\{y^* - \alpha_j\widehat{\theta}_{j-1}\} - (y^* - \alpha_j\theta)$. By (3) and (12), it can be seen that

$$\begin{aligned} J_k &= \frac{1}{k}\sum_{j=1}^{k}(y_j-y^*)^2 \\ &= \frac{1}{k}\sum_{j=1}^{k}(\Delta_j+d_j)^2 \\ &= \frac{1}{k}\sum_{j=1}^{k}d_j^2 + 2\cdot\frac{1}{k}\sum_{j=1}^{k}\Delta_j d_j + \frac{1}{k}\sum_{j=1}^{k}\Delta_j^2. \end{aligned} \tag{21}$$

From (7) and (12), we know that u_k is $\mathscr{F}_{k-1}$-measurable and $|u_k| \leqslant \frac{P_{\max}}{M}$. According to Theorem 1, $\widehat{\theta}_k \to \theta$, w.p.1 $k\to\infty$. Since Eq. (10) is compatible with (11), one can have $\Delta_j \to 0$, a.s. $j\to\infty$. Thus, it follows that

$$\frac{1}{k}\sum_{j=1}^{k}\Delta_j^2 \to 0 \quad \text{a.s.} \quad k\to\infty. \tag{22}$$

Since Δ_j is $\mathscr{F}_{j-1}$-measurable, we have $\mathrm{E}[\Delta_j d_j|\mathscr{F}_{j-1}] = \Delta_j\mathrm{E}[d_j|\mathscr{F}_{j-1}] = 0$, which means that $\{\Delta_j d_j, \mathscr{F}_j\}$ is an MDS. Owing to $\sup_j|\Delta_j| \leqslant \frac{P_{\max}}{M} + |y^*| + \overline{\alpha}\overline{\theta}$, it is known that

$$\sum_{j=1}^{\infty}\frac{\mathrm{E}(\Delta_j d_j)^2}{j^2} \leqslant \sum_{j=1}^{\infty}\frac{(\sup_j|\Delta_j|)^2\mathrm{E}d_j^2}{j^2} \leqslant \left(\frac{P_{\max}}{M}+|y^*|+\overline{\alpha}\overline{\theta}\right)^2\sigma^2\sum_{j=1}^{\infty}\frac{1}{j^2} < \infty.$$

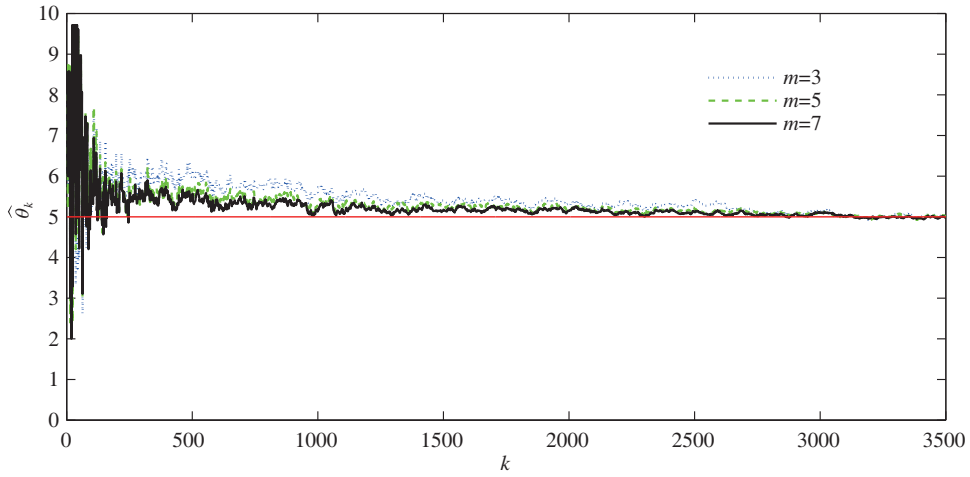

Figure 2 (Color online) Convergence of the identification algorithm.

By Lemma 4, it is obtained that

$$\frac{1}{k}\sum_{j=1}^{k}\Delta_j d_j \to 0, \quad k\to\infty. \tag{23}$$

Note that $\frac{1}{k}\sum_{j=1}^{k} d_j^2 \to \sigma^2$, $k\to\infty$. Owing to (21)–(23), the proof is completed.

5 Numerical simulation

Consider a drag-free satellite, where the mass $M = 1000$ kg, the maximum thrust $P_{\max} = 2\times 10^{-2}$ N, the minimum thrust $P_{\min} = 1\times 10^{-3}$ N, the standard deviation of system noise is 1×10^{-6} N, the speed has a lower bound $\underline{v} = 7.7\times 10^3$ m/s and an upper bound $\overline{v} = 7.9\times 10^3$ m/s, and the measurement range of the gravity gradiometer is $[-6\times 10^{-6}\ \text{m/s}^2, 6\times 10^{-6}\ \text{m/s}^2]$. To avoid round-off error caused by the computer, we multiply (2) by 10^7 and set $\alpha = -\frac{v^2}{2M\times 10^3}$, $\theta = C\rho S\times 10^3$. Therefore, the simulation takes $\sigma = 10$, $\underline{y} = -60$, $\overline{y} = 60$, which means $y^* = 0$, $\underline{\alpha} = -\frac{(7.9\times 1000)^2}{2\times 1000\times 1000}$, $\overline{\alpha} = -\frac{(7.7\times 1000)^2}{2\times 1000\times 1000}$, the constraint set for u_k is $U = [\frac{1\times 10^{-2}}{1000}\times 10^7, \frac{1\times 10^{-3}}{1000}\times 10^7] = [10, 200]$. Assume that $\alpha_k \sim \mathcal{U} = [\underline{\alpha}, \overline{\alpha}]$, $\theta = 5$, $\underline{\theta} = 1$, $\overline{\theta} = 10$, i.e., $\Theta = [1, 10]$.

5.1 Simulation of the identification algorithm for the open-loop system

Suppose that u_k obeys a uniform distribution on U. The influence of m on the algorithm is simulated. We divide the interval $[\underline{y}, \overline{y}]$ into two equal parts, four equal parts, and six equal parts respectively, and then the identification algorithm (7)–(9) is obtained for the case of $m = 3, 5, 7$, where the initial value is $\widehat{\theta}_0^{\{i\}} = 8$, $\nu_i = \frac{1}{m}$, $\beta_i = 12$, $i = 1, \ldots, m$. Figure 2 illustrates the convergence of the algorithm. Figure 3 shows the convergence rate of the algorithm. It can be seen that $k(\widehat{\theta}_k - \theta)^2/\log k$ is bounded, which means $(\widehat{\theta}_k - \theta)^2 = O(\frac{\log k}{k})$. In addition, we can see that the convergence rate of the algorithm is getting faster as m becomes larger.

Replacing $\widehat{\theta}_{k-1}^{\{i\}}$ by $\widehat{\theta}_{k-1}$ in (8) and (9), Figure 4 shows the convergence of the cross-updated algorithm. For $m = 5$, Figure 5 compares the convergence rate of the cross-updated algorithm with the one of the original algorithm. As we expected, the cross-updated algorithm has a faster convergence rate.

5.2 Performance simulation for the closed-loop system

For the closed-loop system under the adaptive control law (12), Figure 6 displays the convergence of the identification algorithm (7)–(9) in three cases of $m = 3, 5, 7$, where the division of $[\underline{y}, \overline{y}]$ and the initial value are the same as above. In Figure 7, it can be seen that $\frac{1}{k}\sum_{j=1}^{k}(y_j - y^*)^2 \to \sigma^2 = 100$, which illustrates the asymptotic optimality of the adaptive controller, which is consistent with Theorem 3.

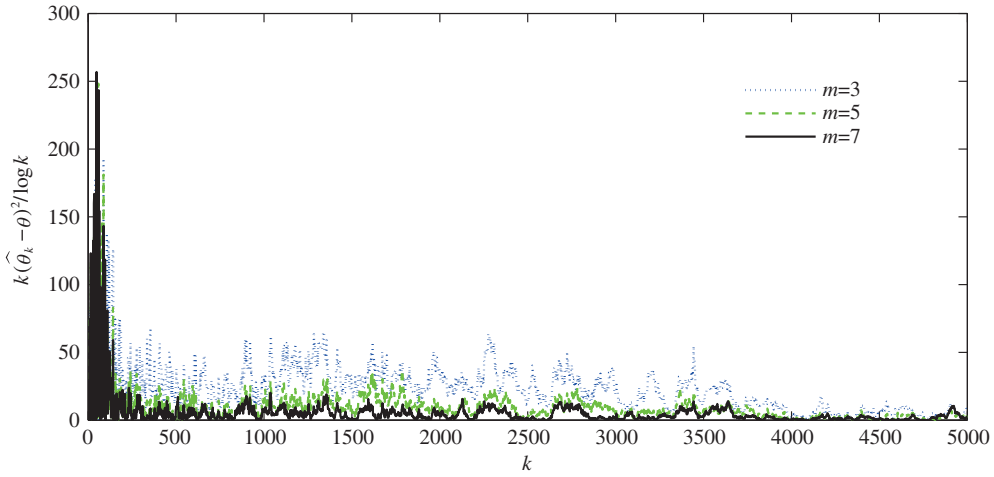

Figure 3 (Color online) Convergence rate of the identification algorithm.

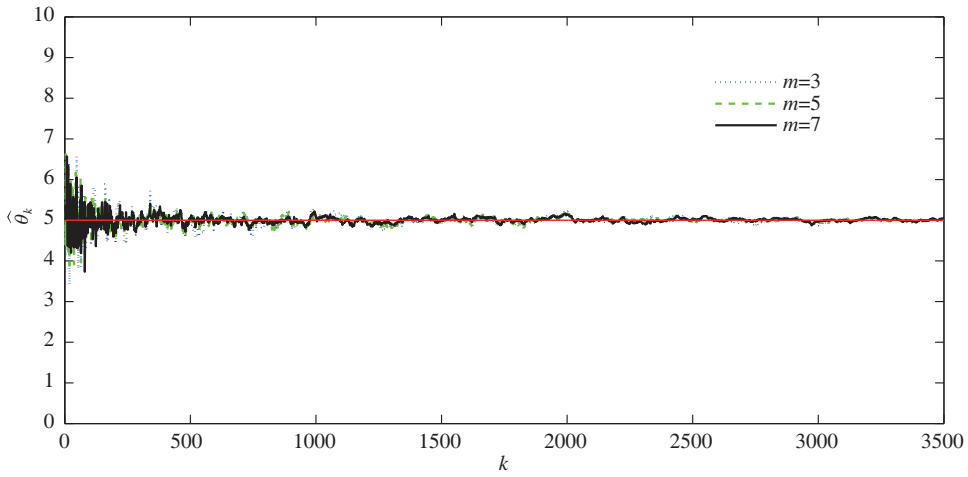

Figure 4 (Color online) Convergence of the cross-updated algorithm.

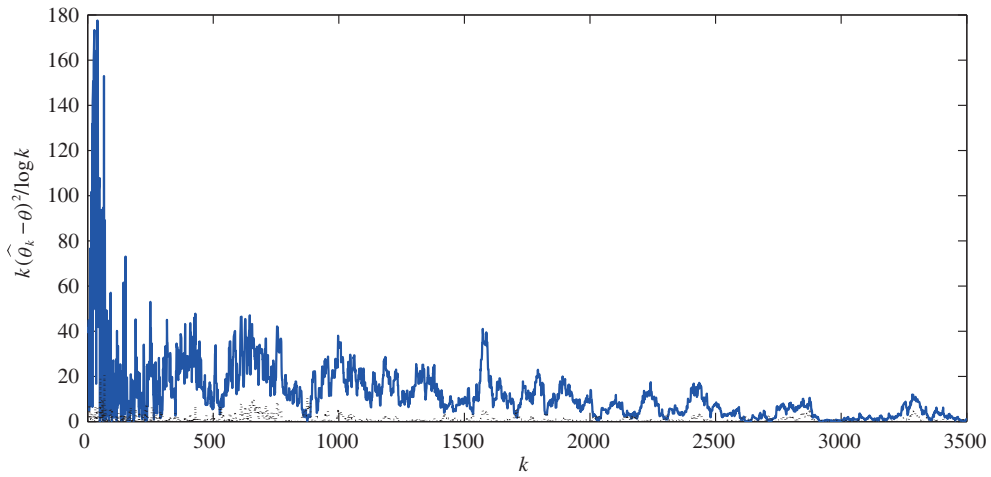

Figure 5 (Color online) Cross-updated algorithm vs. original algorithm ($m = 5$): the solid blue line represents the convergence rate of the algorithm (7)–(9), the black dotted line represents the convergence rate of the cross-updated algorithm.

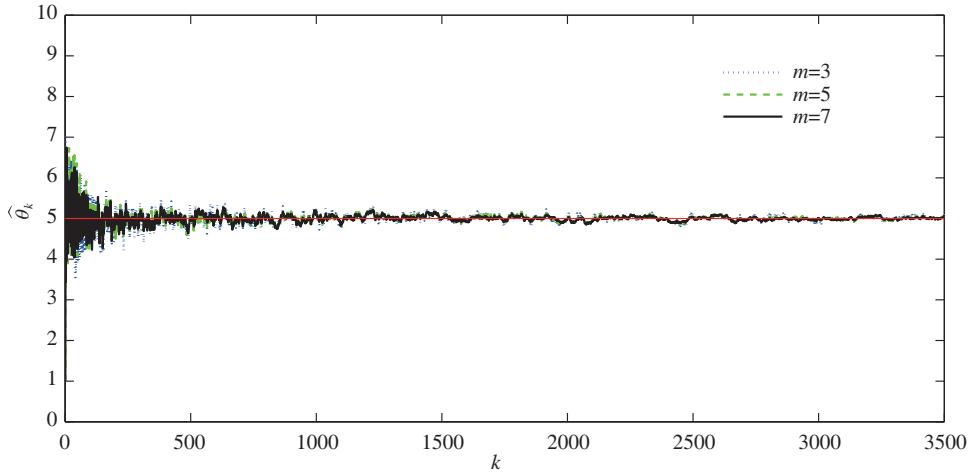

Figure 6 (Color online) Convergence of the identification algorithm in the close-loop system.

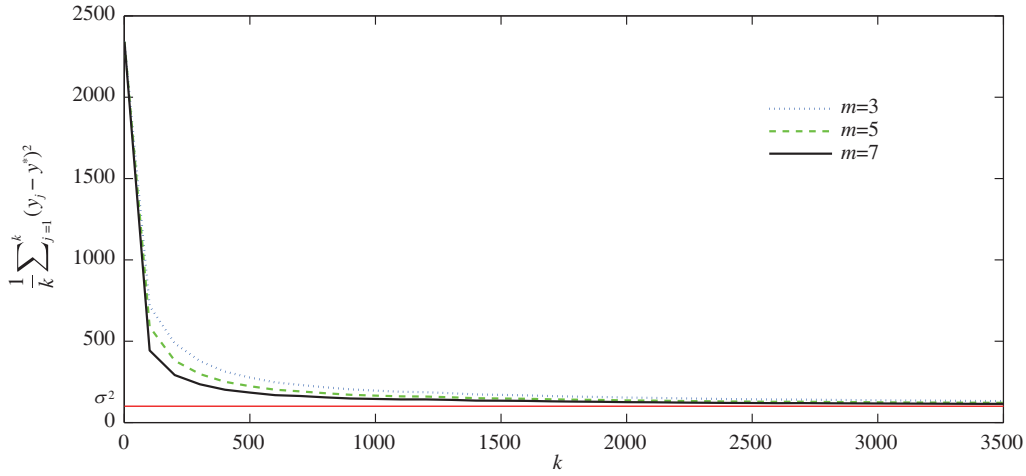

Figure 7 (Color online) Asymptotic optimality of the control law.

6 Conclusion

To resolve the problem of saturation-constrainted observations in the drag-free control technology, this paper introduces a set-valued-identification-based approach to design the adaptive control law. Firstly, by setting several thresholds in the constrained interval, the observation is transformed into set-valued information under different thresholds. Secondly, estimation algorithms for unknown parameters are designed based on set-valued information provided by every threshold, and they are weighted to generate an integrated algorithm. Finally, the adaptive drag-free controller is designed according to the certainty equivalence principle. The performance of the parameter estimation algorithm and the closed-loop system is discussed. There are still many other problems worth studying, such as the cases of high-order system models (the adaptive control in multiple directions), quantized inputs, error-in-variable identification, and colored noise.

Acknowledgements This work was supported by National Key Research and Development Program of China (Grant No. 2018YFA0703800) and National Natural Science Foundation of China (Grant Nos. 61773054, 62025306).

References

1 Dittus H, Lammerzahl C, Turyshev S. Lasers, Clocks, and Drag-Free: Exploration of Relativistic Gravity in Space. Berlin: Springer, 2008
2 Luo Z, Zhong M, Bian X, et al. Mapping Earth's gravity in space: review and future perspective. Adv Mech, 2014, 44: 291–337
3 Lange B. The control and use of drag-free satellites. Dissertation for Ph.D. Degree. Stanford: Stanford University, 1964
4 Haines R. Development of a drag-free control system. In: Proceedings of the 14th Annual AIAA/USU Conference on Small Satellites, Utah, 2000

5 Evers W. GOCE Dynamical Analysis and Drag-Free Mode Control. DCT Report, 2004
6 Canuto E. Drag-free and attitude control for the GOCE satellite. Automatica, 2008, 44: 1766–1780
7 Prieto D, Bona B. Orbit and attitude control for the European satellite GOCE. In: Proceedings of IEEE Networking, Sensing and Control, Politecnico di Torino, 2005
8 Wu S F, Fertin D. Spacecraft drag-free attitude control system design with quantitative feedback theory. Acta Astronaut, 2008, 62: 668–682
9 Prieto D, Ahmad Z. A drag free control based on model predictive techniques. In: Proceedings of American Control Conference, Portland, 2005
10 Yang F, Tan S, Xue W, et al. Extended state filtering with saturation-constrainted observations and active disturbance rejection control of position and attitude for drag-free satellites (in Chinese). Acta Autom Sin, 2020, 46: 2337–2349
11 Guo L, Chen H-F. The Aström-Wittenmark self-tuning regulator revisited and ELS-based adaptive trackers. IEEE Trans Automat Contr, 1991, 36: 802–812
12 Arabi E, Yucelen T. Set-theoretic model reference adaptive control with time-varying performance bounds. Int J Control, 2019, 92: 2509–2520
13 Xiao S, Dong J. Robust adaptive fault-tolerant tracking control for uncertain linear systems with time-varying performance bounds. Int J Robust Nonlin Control, 2019, 29: 849–866
14 Casini M, Garulli A, Vicino A. Input design in worst-case system identification using binary sensors. IEEE Trans Automat Contr, 2011, 56: 1186–1191
15 Godoy B I, Goodwin G C, Agüero J C, et al. On identification of FIR systems having quantized output data. Automatica, 2011, 47: 1905–1915
16 Guo J, Diao J-D. Prediction-based event-triggered identification of quantized input FIR systems with quantized output observations. Sci China Inf Sci, 2020, 63: 112201
17 Zheng C, Li L, Wang L Y, et al. How much information is needed in quantized nonlinear control? Sci China Inf Sci, 2018, 61: 092205
18 Wang L Y, Zhang J F, Yin G G. System identification using binary sensors. IEEE Trans Automat Contr, 2003, 48: 1892–1907
19 Jing L D, Zhang J F. Tracking control and parameter identification with quantized ARMAX systems. Sci China Inf Sci, 2019, 62: 199203
20 Wang T, Bi W, Zhao Y, et al. Radar target recognition algorithm based on RCS observation sequence - set-valued identification method. J Syst Sci Complex, 2016, 29: 573–588
21 Wang L Y, Yin G G, Zhang J F, et al. System Identification with Quantized Observations. Boston: Birkhäuser, 2010
22 You K. Recursive algorithms for parameter estimation with adaptive quantizer. Automatica, 2015, 52: 192–201
23 Lian Y, Luo Z, Weyer E, et al. Parameter estimation with binary observations of input and output signals. In: Proceedings of 2016 Australian Control Conference (AuCC), 2016. 226–231
24 Colinet E, Juillard J. A weighted least-squares approach to parameter estimation problems based on binary measurements. IEEE Trans Automat Contr, 2010, 55: 148–152
25 Zhao Y L, Bi W J, Wang T. Iterative parameter estimate with batched binary-valued observations. Sci China Inf Sci, 2016, 59: 052201
26 Guo J, Zhang J F, Zhao Y L. Adaptive tracking control of a class of first-order systems with binary-valued observations and time-varying thresholds. IEEE Trans Automat Contr, 2011, 56: 2991–2996
27 Guo J, Zhang J F, Zhao Y L. Adaptive tracking of a class of first-order systems with binary-valued observations and fixed thresholds. J Syst Sci Complex, 2012, 25: 1041–1051
28 Zhao Y L, Guo J, Zhang J F. Adaptive tracking control of linear systems with binary-valued observations and periodic target. IEEE Trans Automat Contr, 2013, 58: 1293–1298
29 Chen H-F. Stochastic Approximation and Its Application. Dordrecht: Kluwer Academic Publishers, 2002
30 Guo L. Time-Varying Stochastic Systems—Stability, Estimation and Control. Changchun: Jilin Science and Technolory Press, 1993
31 Chow Y S, Teicher H. Probability Theory: Independence, Interchangeability, Martingales. 2nd ed. New York: Springer-Verlag, 1997